Background to Lecture Notes.

Parts of this document will be more detailed than you will be examined, provided as a holistic overview of the course for those who require this type of understanding.

External Beam radiotherapy using high energy photon beams produced by a medical linear accelerator is the most common form of radiotherapy, so this will be the main focus of these lectures. We will also look at how planning systems work, the data they use to calculate dose and how to plan with them to achieve the optimal individualised plan. We may also touch on kV and electron beam radiotherapy and imaging used in radiotherapy depending on time.

Background Physics

X-ray production.

Bremsstrahlung Radiation - *continuous*.

Electrons rapidly de accelerate by close encounters with an **atomic nucleus** and will radiate some of their kinetic energy as EM wave. All emitted photon energy is about equal intensity. Most electrons don't come close enough to emit x-ray photons and loose energy gradually through many collisions with electrons on the target. Therefore, in the next layer of target material the incoming electrons will have a bit less energy than in the first layer and consequently produce x-rays with similarly flat spectrum, but lower higher energy cut off.

- Photons with energies ranging from zero to the kinetic energy of the incident electron may be produced, resulting in a continuous bremsstrahlung spectrum;
- The bremsstrahlung spectrum produced in a given X ray target depends on the kinetic energy of the incident electron as well as on the thickness and atomic number Z of the target.

Characteristic

Electrons may interact with tightly bound atomic electrons. If internal electron has enough energy to remove, say, a k shell electron then another electron will 'drop' into the vacancy produced by emitting a photon characteristic of the atom. For an ejected k shell electron, l -> k shell transition is most likely and is called a k α photon. Discrete spikes in the spectrum appear for characteristic radiation in the x-ray spectrum. Only present if incident electron beam energy > k shell binding energy.

Interaction probability

Probability is proportional to the cross section (σ) for that interaction

Cross section = notional 'sensitive area' associated with each atom. If hit then interaction will happen.

μ = probability of interaction per unit distance (attenuation coefficient).

$\mu = n \sigma$

n = number of targets = NAdx

total area need to hit = NAdx σ

probability of hitting target of thickness dx = NAdx σ /A = A.dx σ

<u>Photon Interactions</u>

1. Compton – outer electrons (can treat as free as binding energy ~ 10MeV) – scatter photon and loses energy in interaction. T = E(γ -γ ') – mc^2
2. Photoelectric (PE) – inner electron and photon is absorbed. Liberated electron have kinetic energy = T = difference between Binding energy and incident photon energy. To conserve momentum, atomic nucleus recoils.
3. Pair production – photon energy converted into electron-positron pair. Total energy = incident photon energy minus $2mc^2$ (1.022MeV). Annihilation causes back to back photons of 0.511MeV.

The probability of PE increases with proximity of atomic nucleus. $\sigma_{PE\ is}$ proportional to Z^4/E^3 where, Z is atomic number of material (tissue, bone, water) and E is energy.

Mass attenuation coefficient = μ/ρ where ρ = density of material, ρ proportional to Z.

Interaction	Proportional to	μ/ρ
PE		Z^3/E^3
Compton		Constant

$\mu_{total} = \mu_{PE} + \mu_C$

μ_{PE}/ρ proportional Z^3 so even a small difference in average Z value results in a large variation in attenuation so gives a large contrast between tissues of different densities.

BUT

μ_C/ρ does not depend on Z so little variation in μ_C/ρ from one tissue to another, so little contract.

SO

Better contrast with PE so imaging with lower energy x-rays is better, however, this give potentially a higher radiation dose and fewer photons in image when energy so low so higher energy x-rays are better?

Low energy x-ray = soft (more likely to interact)

High energy x-ray = hard.

As x-rays travel through medium low energy x-rays are more likely to interact and be absorbed which leads to filtering the energy spectrum and the average energy of the spectrum increases with filtration, but intensity decreases. **This is called beam hardening, filtered x-rays are more penetrating.**

d*I* = -N σIdx, I = intensity (photons per second), N = atomic density of material, dX = thickness of material, σ is total interaction cross section per atom of material.

Dose to patient relative to initial intensity, I_0.

Dose = $\mu I_0/\rho$

CT imaging for planning

Motivation of CT is to reveal subtle contrast between tissue and allows better anatomical location. Require penetrating x-rays to pass through thickest part of the patient ~ 120keV.

Different density materials attenuate each x-ray by a different amount. This gives us an image and also a value at each pixel to determine how the treatment x-rays will interact in the patient. This allows for a dose calculation at every point.

CT images do not display linear attenuation correction directly, instead display CT numbers or Hounsfield Units (HU) .

$$HU = \left(\frac{\mu(\text{tissue})-\mu(\text{water})}{\mu(\text{water})}\right) x\, 1000,$$

where, $\mu(\text{water}) = 1\ and\ \mu(\text{air}) = 0$

In radiotherapy treatment planning the relative electron density at a point in the patient is used as input into the dose calculation. The TPS (treatment planning systems) use variety of correction techniques for dealing with density heterogeneities, ranging from 1D methods such as effective depth (ratio of tissue maximum ratios (TMRs)) algorithm and the power law algorithm, to methods based on separation of primary and scatter, kernel convolution or Monte Carlo methods – will address each of these later.

For the kV x-rays used in CT scanners, the Compton effect dominates in low-Z materials such as lung, fat and muscle, but a substantial proportion of the attenuation is PE in higher Z materials such as bone. In the Compton region, μ is almost completely proportional to ρ_e, the electron density relative to water, giving rise to the solid line in figure 3. For bone-like materials, the presence of Calcium leads to the dashed line in figure 3. The slope of the solid line does not vary with energy; however, the slope of the dashed line varies between scanners, and between kV settings on the same scanner.

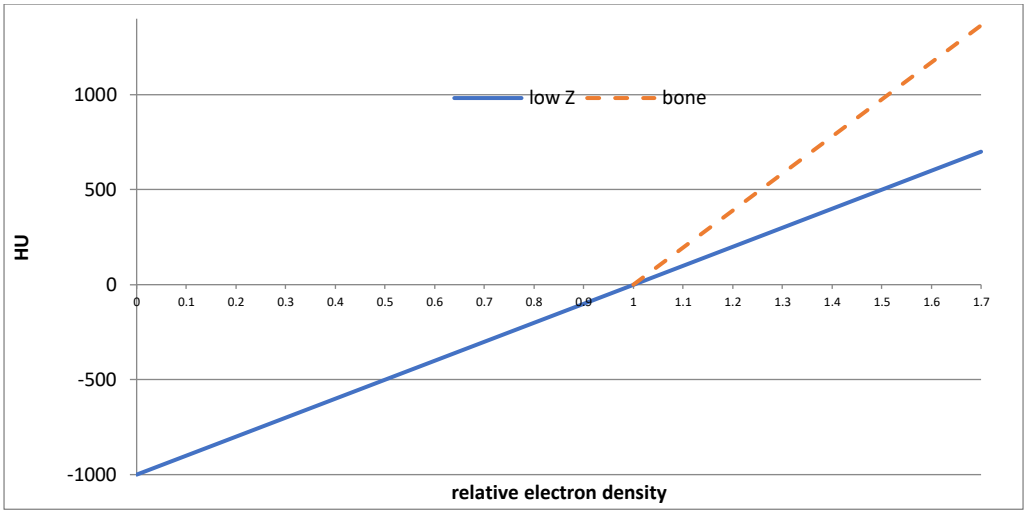

Figure 3.

Since for the MV x-rays used in radiotherapy the dominant attenuation is Compton (even in bone), conversion using figure 3 is all that is required. Each scanner will require calibration of HU to relative electron density using density phantoms of known electron densities to plot the relationship. Though simply relationships can be used such as,

For HU < 100,

$$\rho_e = \frac{HU}{1000} + 1.00$$

For HU > 100

$$\rho_e = \frac{HU}{1950} + 1.00$$

Dose calculation Algorithms (taken from S. Thomas's Scope Tutorial)

Dose deposition in tissue is dominated by charged particle (electron) transport, from electrons released in Compton and other interactions. In a medium that is much less dense than water, such as lung, an electron travels much further before losing its energy. This means that the beam penumbra, measured in a lung phantom, is wider than the penumbra of the same beam measured in a water phantom.

A photon travels in a straight line until it interacts with matter. For a megavoltage photon in tissue or water, the most likely interaction is Compton scattering. The other two major interactions are the Photoelectric Effect (PE) and Pair Production (PP). All three of these involve transfer of energy to an electron, which then deposits dose by ionisation as it travels up to its maximum range. In Compton and PE there is also energy given to a scattered

photon, which will travel a greater distance before possibly interacting to deliver dose at a distance from the first interaction. In PP, the positron deposits dose by ionisation in a similar manner to the electron, before annihilating with an electron to produce two photons of 511 keV, which will contribute to the dose at a distance from the first interaction.

Therefore, a photon interaction leads to dose being deposited over a range of distances and directions, most locally (within the range of the electrons produced), and some at a greater distance (due to secondary photons). The distribution of this can be modelled empirically or by Monte Carlo methods, and used to form the basis of a number of dose calculation techniques, using some form of convolution of the primary interactions with the dose deposition.

Monte Carlo

Anything that picks events from a probability distribution using random numbers is a Monte-Carlo simulation. In the context of this tutorial, we will restrict this to following the interactions of photons and electrons. In principle, this can be done by knowing the probabilities of all the interaction processes (PE, Compton, PP etc.) for all energies in a particular material, and the probability distribution for angular distribution of scattered photon, Compton electron etc. Using random numbers, one can decide the distance to next interaction, type of interaction etc. The same should be done for all the secondary particles produced until all the energy is absorbed. The process is then repeated for enough histories to give an acceptable statistical uncertainty.

However, electrons are very densely ionising. The mean free path between collisions is tiny. As a result, far too many calculations are needed to follow them, so approximations are used to make calculations manageable. Different MC codes make different assumptions to increase speed, with the result that we are no longer being true to the laws of physics, but making the same trade-offs between speed and accuracy that we find in other algorithms. MC calculations are subject to statistical uncertainty in dose, proportional to $1/\sqrt{N}$, where N is the number of histories. As a result, calculations need large numbers of histories (of the order of 10^4 per voxel to get down to 1%).

The process of calculating a dose, from linac to patient, is as follows:

1. Start with an electron exiting from waveguide
2. Follow it and its descendants through targets, primary collimators, ion chambers etc.
3. Track it through patient dependant structures (jaws, MLC etc.)
4. Track it through the patient (as modelled from CT data set)

MC planning systems can speed up the process by pre-calculating to end of (2) and storing a phase-space file. Several commercial systems (e.g. Monaco, BrainLab and RayStation) use code based on the Voxel Monte Carlo (VMC) [6,7] code and code derived from it such as XVCM and VMC++. Eclipse uses Macro Monte Carlo (MMC)[8] for electron calculations. These codes give much faster calculations than those based on generalised Monte Carlo codes, at a price of introducing a number of simplifying approximations.
Where a general MC code such as EGS4 or EGSnrc[9] is designed to describe electron transport in a wide range of energies and materials, for arbitrary geometries, VMC restricts

itself to electrons with kinetic energy 1 to 30 MeV, and to low Z materials with densities of 0 to 3 kg m^{-3}, and only performs dose calculations in rectangular geometries (as defined by the patient CT image). VMC also uses a simplified version of the distribution for multiple scattering, and uses energy cut-offs (typically 500 keV for electrons, 50 keV for photons) to increase speed. MMC speeds calculations by transporting electrons in large-scale macroscopic steps through the absorber.

Most of the convolution/superposition algorithms (see next section), use Monte-Carlo calculations to generate kernels showing how the dose from a single photon interaction is deposited in water.

Convolution/superposition algorithms

Since the average energy required to produce an ion pair is approximately 35eV, and the energy transferred to an electron in a photon interaction will be of the order of MeV, it will be seen that there are tens of thousands of electron interactions to each photon interaction. Practically all the dose that is deposited is from ionisation by electrons. When considering the dose deposited per photon interaction in the primary beam, it is necessary also to consider the long-range dose deposition from secondary photons (which will themselves transfer energy to electrons when they interact with matter).
Unlike in dosimetry, where KERMA (Kinetic Energy Released per unit mass) is used, in treatment planning algorithms it is more common to use TERMA (Total Energy Released per unit mass). KERMA considers the energy transferred to electrons, and excludes the energy given to secondary photons. TERMA includes all the energy removed from the primary beam.
The calculation of TERMA in a patient requires the following:

- The attenuation coefficient μ for each point in the patient. This will depend on:
  - The energy spectrum of the radiation
  - The electron density at each point (which can be calculated from the CT values).
- Strictly you also need the physical density (since TERMA is proportional to μ/ρ); some vendors assume that tissue is scaled water.
- The geometrical penumbra; this is allowed for by convolving with one or more gaussians.

The energy is transferred to electrons (which deposit energy over a short range) and to secondary photons (which deposit their energy over a larger range). It is possible to use Monte Carlo modelling to produce a "dose deposition kernel" giving the spatial distribution in 3D of a the dose deposition that results from a the loss of energy at a given point.

To calculate dose in an homogenous medium, $D=T \otimes K$ (Dose = Terma convolved with Kernel), it will be seen that convolution requires an invariant kernel. In other words, the width of the kernels used to blur the dose distribution does not vary with position. This is fine in a water tank. However in a patient, where the electron density varies, we have seen that the width of the kernel varies also. This means that algorithms that rely on FFT convolutions cannot model the variation of penumbra with density.

Linear Boltzmann transport equations

The most recent class of algorithms to make it into a commercial system is based on solutions of the linear Boltzmann transport equation (LBTE). The Boltzmann transport equation (BTE) describes the behaviour of photons and particles as they pass through and interact with matter. The non-linear form of the equation can model interactions of one particle with another, whilst the linear form assumes the photons and particles only interact with the matter they are passing through.

Unlike Monte Carlo, which uses random numbers to follow histories, numerical methods to explicitly solve the LBTE are used. In principal, both Monte Carlo and LBTE methods should converge to the same answer if all computational approximations are removed and enough time is allowed for calculation, since they will both be limited by the same uncertainties in the particle interaction data. In practice, both methods use approximation to speed up calculations, so neither is exact. LBTE is more prone to systematic errors from the fact that a continuously variable function is cut up into discrete steps of position, energy and angle, whilst Monte Carlo is more prone to random errors from insufficient numbers of histories being used.

How a Linac works

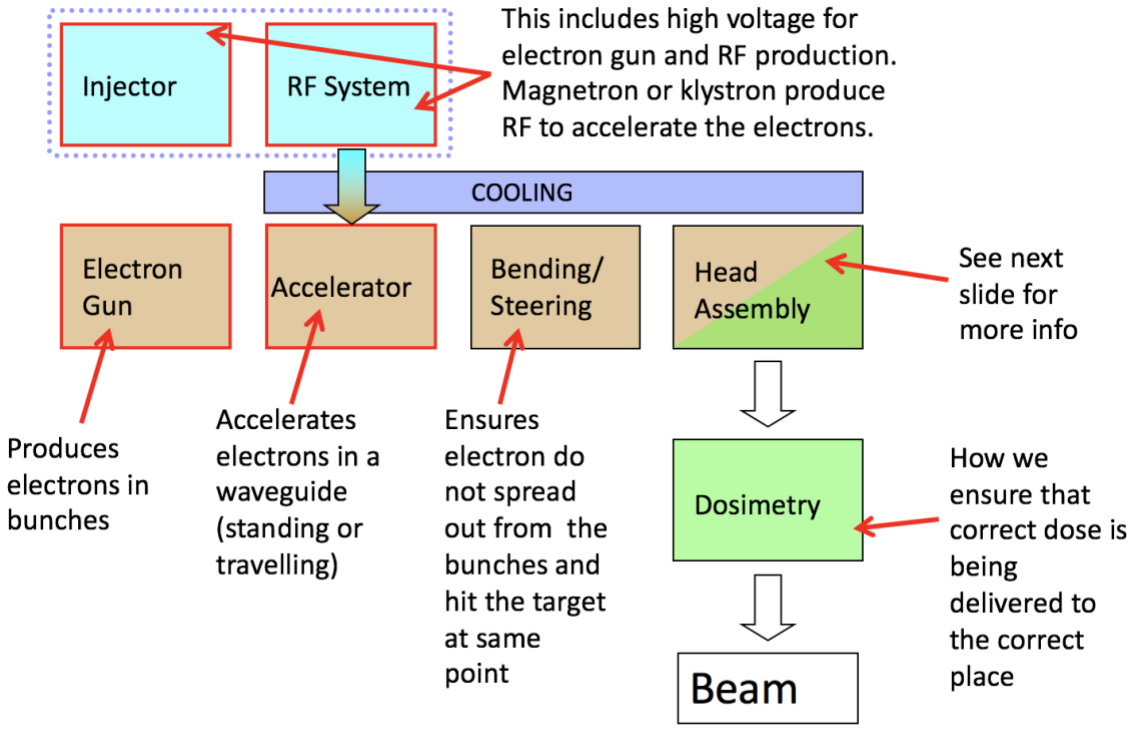

The electron gun

The electron gun creates a stream of electrons that are fed into the waveguide to meet microwaves produced by the RF generator. These electrons are thermionically emitted from a cathode.

The radio frequency generator

Two types of generators are used in LINACs, the Magnetron and the Klystron. All we really need to know here is that they essentially perform the same task: they produce RF waves of about 3 GHz to drive the accelerator waveguide.

The accelerating waveguide

The RF source emits the RF wave at a rate of several hundred pulses per second, and this is fed into the waveguide in synchrony with the electrons. As an electromagnetic wave will travel at the velocity of light (c) in free space, in order to position the electrons on the part of the wave where they will experience the maximum force (wave crest), it is necessary to slow down the RF wave at the beginning of the guide. This is achieved by placing a series of iris diaphragms along the length of the internal aspect of the guide, the spacing and lumen diameter of these will control the speed of the wave.

The principles of acceleration are different in each of the following waveguide designs:

- Travelling waveguide.
- Standing waveguide.

Some differences between a travelling and a standing waveguide are:

- Standing waveguides produce higher accelerating gradients. Traveling waveguides will have a lower rate of electrons acceleration as the electron 'ride' the RF wave in the travelling wave guide.

- The standing waveguide is a highly resonant system and functions efficiently at a fixed frequency. A result of this fixed frequency is a stable energy output.

The treatment head

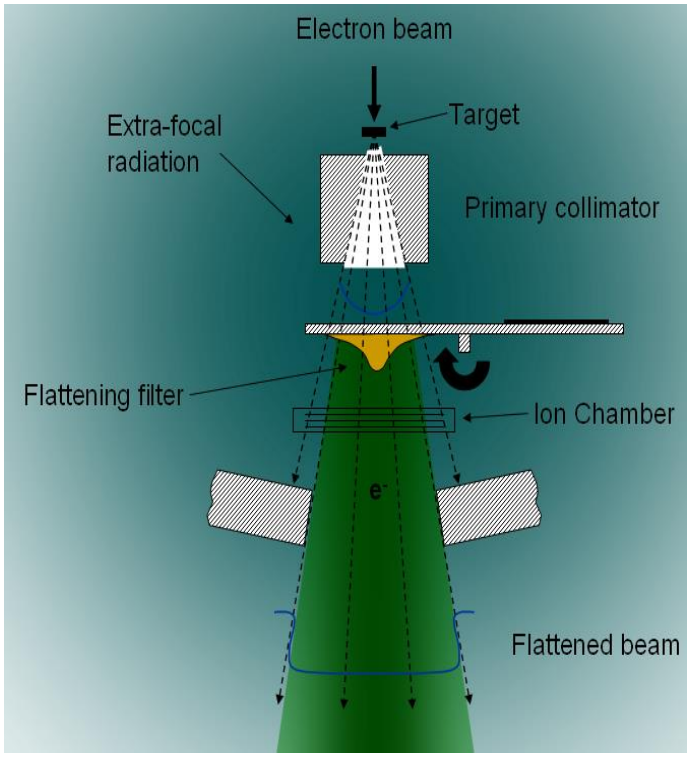

After the electron beam has been bent by the bending magnet, the electrons travel to the treatment head which has the following components:

The Target

It is a retractable piece of tungsten (energies ≤ 10 MeV) or gold alloy (energies > 10 MeV) which the electron beam strikes. The resulting X-ray beam has a continuous spectrum, which matches the minimum and the maximum energies of the incident electrons.

The primary collimator

It is a lead cone-shaped block which defines the maximum field size available for clinical treatment.

The beam flattening filter (note newer Linacs may not use this in IMRT or SABR)

It is a conical metal filter situated between the target and the ionisation chamber. It is thickest at the centre in order to produce a uniform intensity distribution over the central axis of the beam, where the X-rays leaving the target present an energy peak.

The ionisation chamber

The dual ionisation chamber system, which samples points across the treatment beam, will terminate the treatment when the prescribed dose has been given, or if the energy, quality, flatness, symmetry or dose rate of the emitted beam falls outside normal operating parameters. The two chambers operate independently of each other in case one should fail, and are sealed ion chambers to prevent variations in the sensitivity of response because of fluctuations in temperature and pressure. The chambers are divided into segments. In some designs the central segment monitors dose and dose rate. The two outer segments are used as

dose comparators across the beam profile. In general, the greater the number of segments into which the chambers are divided, the more detailed the information received.

Secondary Collimators

Once the radiation has left the ion chamber, its field size is controlled by secondary collimators that are thick enough to absorb 98% of the main beam. The secondary

collimators are usually constructed of a high density material such as lead or tungsten alloy and are mounted in pairs either side of the central axis of the beam. Various problems can arise from the secondary collimators:

1. (a) They can produce significant amounts of secondary electrons, which if the patient is close to the treatment head, can impair the skin sparing effect.
2. (b) The closer the collimator is to the target within the treatment head, the larger the geometric penumbra in the isocentric plane. Secondary collimators are designed to reduce the penumbra to a minimum by:

    • Being placed as far away as possible from the X-ray source.
    • Matching the shape of the collimator edge to the divergence of the beam.

Wedges

During the planning stage wedges are used to produce the desired isodose profile in order to match the desired treatment volume. In practice, these wedges are leaves or blocks of lead placed in or under the collimator to attenuate the beam to the desired shape. Variable wedges are an integral part of most modern linear accelerators as an alternative to wedges of fixed angles of 15, 30, 45 and 60, which have to be inserted manually into a treatment unit. Variable wedges can be either a single motorised wedge, or virtual wedges when the collimator is driven across the field for a chosen period of time. Wedges are used to produce a satisfactory distribution where beams intersect, so that a high dose area can be avoided. They may also be used to compensate for obliquity of body contour or a sloping target volume. To achieve the same dose at the patient, the number of monitor units set will have to be increased compared with that for an open field.

All the individual components discussed above constitute the skeleton of the gantry of a standard Linac. Together with the gantry, every Linac is composed of other components - such as the couch, collimator rotation and IGRT. All the movements of these components compromise the positional accuracy required to treat patients. In order to achieve a high level of accuracy, all the Linac components will move around a reference point, the isocentre, which remains at the same place during gantry, collimator and couch rotations.

Margins for planning

Besides meeting planning constraints the treatment plan is also required to meet the aims of the planner *at each and every fraction*. The ability to plan and deliver treatments of greater conformality and complexity led to the need for uniform recording, reporting and prescribing to account for geometric uncertainties. An *uncertainty* refers to any variation between the

planned and delivered dose distribution and they arise from the fact that treat- ment plans are based on a static view of a living, and therefore, a very non-static patient. The variation between the planned dose distribution and the delivered dose distribution is a measure of a plan's robustness: the smaller the variation the greater the plan robustness. Residual uncertainties are unavoidable despite efforts in variation reduction such as patient immobilisation and image guided radiotherapy treatment (IGRT) . International Committee on Radiation Units and Measurements (ICRU) Reports 50 and 62 (*ICRU 50*, 1993; *ICRU 62*, 1999) provided a solution by defining target volumes in conventional radiotherapy including.

GTV - Gross Tumour Volume (GTV), the visible tumour

CTV - Clinical Target Volume (CTV), which includes the GTV and microscopic growth

PTV - Planning Target Volume (PTV) which encompasses both the GTV and CTV as well as accounting for any deviations from our static model.

OAR – Organs at Risk

PRV – Analogous to the PTV, a Planning organ at Risk Volume (PRV) is used for Organs at Risk (OAR

A bit more about the PTV

In regard to conventional radiotherapy, *Stroom et al.* (1999) and *van Herk et al.* (2000) suggested that uncertainties fall into two categories, namely preparation and treatment execution uncertainties. Treatment execution uncertainties are random and act to blur the ideal dose distribution by a Gaussian distribution with a width dependent on the photon penumbra and the standard deviation of day-to-day variations in the CTV location. Preparation uncertainties are present at every fraction of the treatment and are therefore systematic in nature. Using the shift invariance assumption, systematic uncertainties result simply in a shift of the dose distribution with the same direction and magnitude.

Van Herk also addressed the problem of how to combine both these types of uncertainty in an analytical model to determine the CTV-PTV margin. It was shown that it was incorrect to combine the standard deviations of the uncertainties linearly due to the lack of correlation between systematic and random uncertainties. It was acknowledged that the systematic uncertainty is stochastic across the patient population. Van Herk's PTV margin for systematic uncertainties is de ned so that the CTV has a 90% chance of being in the PTV. This, now well known, margin recipe (equation 1.1) allows that in 90% of patients treated to meet the ICRU recommendations, the CTV receives at least 95% of the prescribed dose.

$$PTVmargin = 2.5\Sigma + 1.64(\sqrt{(\sigma_p^2 + \sigma^2)}) - 1.64\sigma_p \quad (1.1)$$

where, Σ is the standard deviation of the systematic uncertainty, σ if the standard deviation of the random uncertinaity and σ_p is the unblurred beam penumbra width. In this paper Van Herk (*van Herk et al.*, 2000) suggests rede ning the PTV as,

"The volume in treatment room coordinates to which the prescribed dose must be delivered in order to obtain a clinically acceptable and speci ed probability that the prescribed dose is actually received by the CTV, which has an uncertain location."

In this way uncertainties are condensed into the CTV-to-PTV margin. The *static PTV* represents the *moving CTV* and is therefore a useful method of evaluating a plan, by using Dose Volume Histograms (DVHs) to report the minimum dose to the CTV with a pre-speci ed con dence level. The PTV then becomes a surrogate target for both treatment plan optimi- sation and evaluation.

Planning with a PTV has some limitations; for example it is problematic in cases where the CTV is close to the skin. It is important that there is con dence in quantifying and identifying uncertainties used to grow the PTV margin and that they are speci c for treatment site, modality used, and treatment regime to ensure optimal treatment. In using Image Guided Radiotherapy (IGRT) greater information about the systematic uncertainty can be acquired, allowing for corrections to be made and a reduction in the margins used. IGRT is the use of imaging at pre-treatment and delivery to improve or veri y the accuracy of radiother- apy. IGRT includes methods of simple visual eld alignment checks, to the more complex volumetric imaging that allows direct visualisation of the target volume and surrounding anatomy (*NRIG*, 2012). In the case of online IGRT (where the images are analysed and used on set), information about the random component can be gained and corrected for by applying rigid shifts to the treatment table, aligning either soft tissue or bony landmarks in the daily image to the planning image. This again, allows for a reduction in the CTV to PTV margin. However, if reduced too much the margin may become inadequate and the tumour control probability or other endpoint may worsen, such as biochemicall failure as seen by (*Engels et al.*, 2009). If the margin is too large, greater incidence and severity in normal tissue complication may be seen.

Furthermore, the PTV concept is still present in newer approaches where inhomogeneous doses are prescribed. Such cases are in con ict with several of the underlying assumptions taken in van Herk's original margin design. As a consequence, the indirect estimation of the con dence level becomes unreliable. Intensity modulated particle therapy (IMPT) is one such example, where complex and inhomogeneous dose distributions are delivered, often with steep dose gradients. Along with the extra degree of freedom in the proton range, this renders the PTV an inadequate planning tool. This is partly due to the shift invariance assumption (also known as *static-cloud*) as it cannot be applied to the proton case. This assumption relies

on a rigid isocentric shift of the dose distribution, in the same direction and magnitude as the geometric uncertainty, and is representative of the delivered dose when experiencing the same geometric uncertainty. For example, if a shift, S is applied, this means that the dose value at a voxel D_i, is now $D_{(i-S)}$. The shift invariance relies on assuming the patient contour is unchanged when the dose isocentre is moved and also on the radiation passing through tissue of the same density before and after the dose isocentre shift (*Nguyen et al.*, 2009). The sensitivity of the proton range to density heterogeneities in the traversing material means this assumption can no longer be made. Even if there has been no shift by the patient and no change in the tumour size, shape or positioning there is still an uncertainty due to changes in the radiological path-length, resulting from patient changes such as weight gain or loss.

MV Beam Properties (from Khan)

As the beam is incident on a patient (or a phantom), the absorbed dose in the patient varies with depth. This variation depends on many conditions: beam energy, depth, field size, distance from source, and beam collimation system. Thus the calculation of dose in the patient involves considerations in regard to these parameters and others as they affect depth dose distribution.

An essential step in the dose calculation system is to establish depth dose variation along the central axis of the beam.
One way of characterizing the central axis dose distribution is to normalize dose at depth with respect to dose at a reference depth. The quantity *percentage* (or simply *percent*) *depth dose* may be defined as the quotient, expressed as a percentage, of the absorbed dose at any depth *d* to the absorbed dose at a fixed reference depth d_0, along the central axis of the beam (Fig. 9.2). Percentage depth dose (*P*) is thus:

$$P = \frac{D_d}{D_{d_0}} \times 100 \qquad (9.3)$$

In clinical practice, the peak absorbed dose on the central axis is sometimes called the *maximum dose*, the *dose maximum*, the *given dose*, or simply the D_{max}. Thus,

$$D_{max} = \frac{D_d}{P} \times 100 \qquad (9.4)$$

A number of parameters affect the central axis depth dose distribution. These include beam quality or energy, depth, field size and shape, source to surface distance, and beam collimation. A discussion of these parameters will now be presented.
A. Dependence on Beam Quality and Depth

The percentage depth dose (beyond the depth of maximum dose) increases with beam energy. Higher-energy beams have greater penetrating power and thus deliver a higher percentage depth dose (Fig. 9.3). If the effects of inverse square law and scattering are not considered, the percentage depth-dose variation with depth is governed approximately by exponential attenuation.

A.1. Initial Dose Build-Up

As seen in Fig. 9.3, the percentage depth dose decreases with depth beyond the depth of maximum dose. However, there is an initial buildup of dose which becomes more and more pronounced as the energy is increased. In the case of the orthovoltage or lower-energy x-rays, the dose builds up to a maximum on or very close to the surface. But for higher-energy beams, the point of maximum dose lies deeper into the tissue or phantom. The region between the surface and the point of maximum dose is called the *dose build-up region*. The dose build-up effect of the higher-energy beams gives rise to what is clinically known as the *skin-sparing effect*. For megavoltage beams such as cobalt-60 and higher energies the surface dose is much smaller than the D_{max}. This offers a distinct advantage over the lower-energy beams for which the D_{max} occurs at the skin surface. Thus, in the case of the higher energy photon beams, higher doses can be delivered to deep-seated tumors without exceeding the tolerance of the skin. This, of course, is possible because of both the higher percent depth dose at the tumor and the lower surface dose at the skin. This topic is discussed in greater detail in Chapter 13.

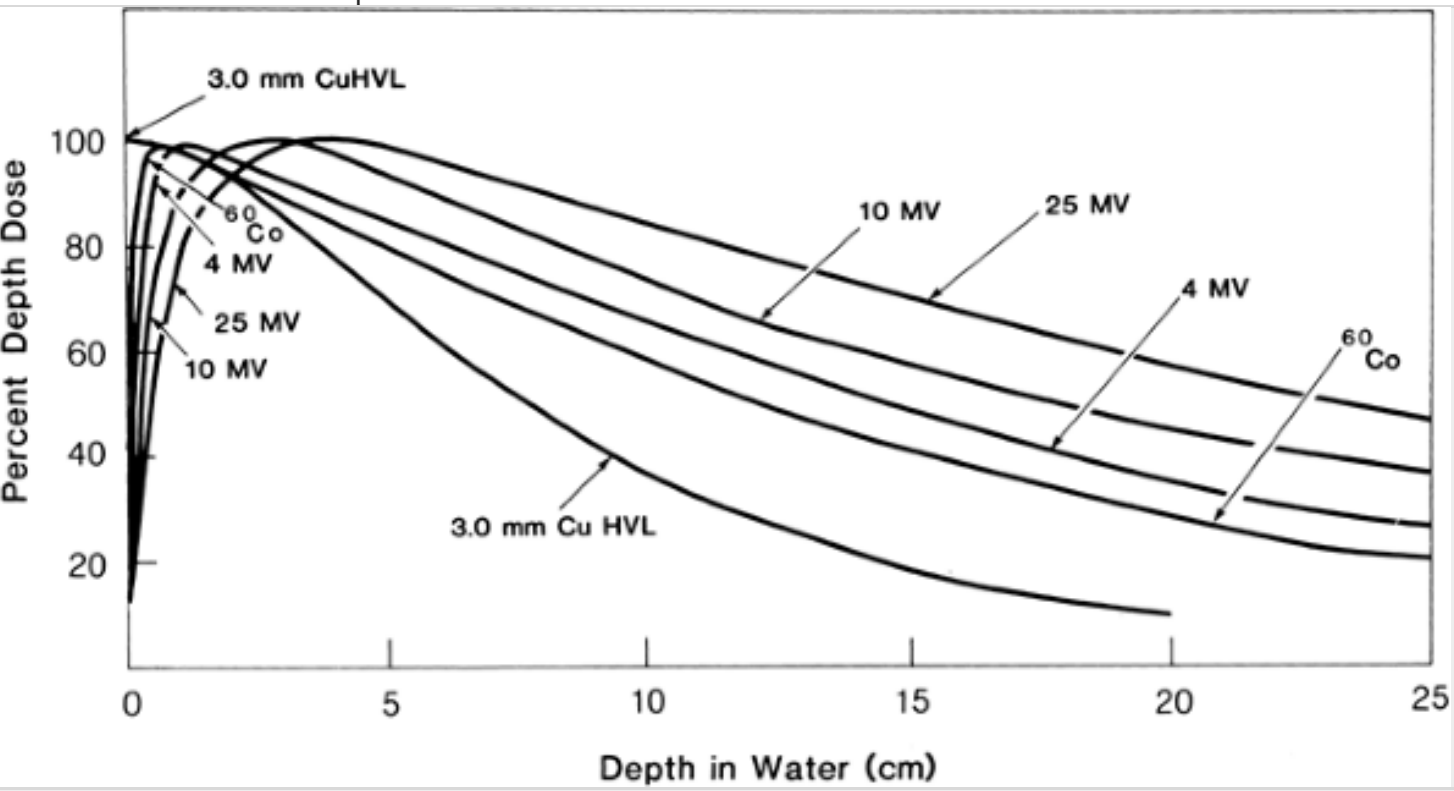

FIG. 9.3. Central axis depth dose distribution for different quality photon beams. Field size, 10 Ã— 10 cm; SSD = 100 cm for all beams except for 3.0 mm Cu HVL, SSD = 50 cm. (Data from Hospital Physicistsâ€™ Association. Central axis depth dose data for use in radiotherapy. *Br J Radiol* 1978;[suppl 11]; and the Appendix.)

The physics of dose buildup may be explained as follows: (a) As the high-energy photon beam enters the patient or the phantom, high-speed electrons are ejected from the surface and the subsequent layers; (b) These electrons deposit their energy a significant distance away from their site of origin; (c) Because of (a) and (b), the electron fluence and hence the absorbed dose increase with depth until they reach a maximum. However, the photon energy fluence continuously decreases with depth and, as a result, the production of electrons also decreases with depth. The net effect is that beyond a certain depth the dose eventually begins to decrease with depth.

Effect of Field Size and Shape

Field size may be specified either geometrically or dosimetrically. The geometrical field size is defined as â€œthe projection, on a plane perpendicular to the beam axis, of the distal end of the collimator as seen from the front center of the sourceâ€• (15). This definition usually corresponds to the field defined by the light localizer, arranged as if a point source of light were located at the center of the front surface of the radiation source. The dosimetric, or the physical, field size is the distance intercepted by a given isodose curve (usually 50% isodose) on a plane perpendicular to the beam axis at a stated distance from the source. Unless stated otherwise, the term field size in this book will denote geometric field size. In addition, the field size will be defined at a predetermined distance such as the source-surface distance (SSD) or the source-axis distance (SAD). The latter term is the distance from the source to axis of gantry rotation known as the isocenter.

For a sufficiently small field one may assume that the depth dose at a point is effectively the result of the primary radiation, that is, the photons which have traversed the overlying medium without interacting. The contribution of the scattered photons to the depth dose in this case is negligibly small or 0. But as the field size is increased, the contribution of the scattered radiation to the absorbed dose increases. Because this increase in scattered dose is greater at larger depths than at the depth of Dmax, the percent depth dose increases with increasing field size.

The increase in percent depth dose caused by increase in field size depends on beam quality. Since the scattering probability or cross-section decreases with energy increase and the higher-energy photons are scattered more predominantly in the forward direction, the field size dependence of percent depth dose is less pronounced for the higher-energy than for the lower-energy beams.

Percent depth dose data for radiation therapy beams are usually tabulated for square fields. Since the majority of the treatments encountered in clinical practice require rectangular and irregularly shaped (blocked) fields, a system of equating square fields to different field shapes is required. Semiempirical methods have been developed to relate central axis depth dose data for square, rectangular, circular, and irregularly shaped fields. Although general methods (based on Clarkson's principleâ€”to be discussed later in this chapter) are available, simpler methods have been developed specifically for interrelating square, rectangular, and circular field data.

Dependence on Source-Surface Distance

Photon fluence emitted by a point source of radiation varies inversely as a square of the distance from the source. Although the clinical source (isotopic source or focal spot) for external beam therapy has a finite size, the source-surface distance is usually chosen to be large (â‰¥80 cm) so that the source dimensions become unimportant in relation to the variation of photon fluence with distance. In other words, the source can be considered as a point at large source-surface distances. Thus the exposure rate or â€œdose rate in free spaceâ€• (Chapter 8) from such a source varies inversely as the square of the distance. Of course, the inverse square law dependence of dose rate assumes that we are dealing with a primary beam, without scatter. In a given clinical situation, however, collimation or other scattering material in the beam may cause deviation from the inverse square law.

Percent depth dose increases with SSD because of the effects of the inverse square law. Although the actual dose rate at a point decreases with increase in distance from the source, the percent depth dose, which is a relative dose with respect to a reference point, increases with SSD. This is illustrated in Fig. 9.5 in which relative dose rate from a point source of

radiation is plotted as a function of distance from the source, following the inverse square law. The plot shows that the drop in dose rate between two points is much greater at smaller distances from the source than at large distances. This means that the percent depth dose, which represents depth dose relative to a reference point, decreases more rapidly near the source than far away from the source.
In clinical radiation therapy, SSD is a very important parameter. Because percent depth dose determines how much dose can be delivered at depth relative to the surface dose or Dmax, the SSD needs to be as large as possible. However, because dose rate decreases with distance, the SSD, in practice, is set at a distance which provides a compromise between dose rate and percent depth dose.

Forward Planning

Inverse Planning

In current inverse planning systems for IMRT the dose distribution is determined using a computerised optimisation based on dose objectives for targets and other volumes which have been assigned an importance level. To determine the plan quality, a number is assigned based on the deviation from objective dose for each volume and the optimisation result is the plan with the lowest number.

Limitations

This is a trial and error process, given that the resulting plan may not be clinically acceptable and the importance levels assigned to each volume may need adjusting and the optimisation re-run. This can be time-consuming and the best-quality plan may not have been achieved as the planner cannot try every combination of parameters. There also exists a problem that, if upper and lower constraints are met, the optimisation process will not further improve doses to these volumes.